Supporting Information

O_2 and water migration pathways between the solvent and heme pockets of hemoglobin with open and closed conformations of the distal HisE7

Maria S. Shadrina, Gilles H. Peslherbe and Ann M. English

Department of Chemistry and Biochemistry, Centre for Research in Molecular Modeling and PPOTEO, Concordia University, 7141 Sherbrooke Street West, Montreal, Quebec, Canada, H4B 1R6

E-mails: ann.english@concordia.ca; gilles.peslherbe@concordia.ca

Contents

Table S1. Summary of simulations performed of the six HbA models

TLES HbA model [a]	TLES O_2 location [b]	Number of independent 2-ns simulations [c]	Number of simulated O_2 trajectories	Total time of simulated O_2 diffusion, ns
T_c + 15 TLES O_2	α-subunit	32	480	960
T_o + 15 TLES O_2	α-subunit	32	480	960
T_ + 15 TLES O_2	α-subunit	32	480	960
R_c + 15 TLES O_2	α-subunit	32	480	960
R_o + 15 TLES O_2	α-subunit	32	480	960
R- + 15 TLES O_2	α-subunit	32	480	960
T_c + 15 TLES O_2	β-subunit	32	480	960
T_o + 15 TLES O_2	β-subunit	32	480	960
T- + 15 TLES O_2	β-subunit	32	480	960
R_c + 15 TLES O_2	β-subunit	32	480	960
R_o + 15 TLES O_2	β-subunit	32	480	960
R- + 15 TLES O_2	β-subunit	32	480	960
Ligand-free HbA model Standard MD simulations [a]		**Number of independent 32-ns simulations [c]**	**Number of simulated trajectories per subunit [d]**	**Total simulation time per subunit, ns [d]**
T_c		15	30	960
T_o		2	4	128
T-		2	4	128
T_{cw}		2	4	128
R_c		15	30	960
R_o		2	4	128
R-		2	4	128
R_{cw}		2	4	128

[a] Crystal structures PDB 2DXM (*1*) and 2DN3 (*2*) were used for the **T** and **R** models, respectively. Wild-type HbA with HisE7 in its neutral, *closed* ($\mathbf{T_c}$, $\mathbf{R_c}$) and protonated, *open* ($\mathbf{T_o}$, $\mathbf{R_o}$) conformations was modeled. The HbA(α,βHisE7Gly) variant represents models with no HisE7 barrier (**T-**, **R-**). $\mathbf{T_c}$ and $\mathbf{R_c}$ were also modeled with a single water molecule occupying their distal heme sites ($\mathbf{T_{cw}}$, $\mathbf{R_{cw}}$).

[b] Fifteen TLES O_2 copies were placed in the distal heme site of the indicated subunit.

[c] Number of independent simulations carried out for each HbA model.

[d] Since HbA contains two α- and two β-subunits each ligand-free simulation of HbA provides two trajectories for the α-subunit and two for the β-subunit.

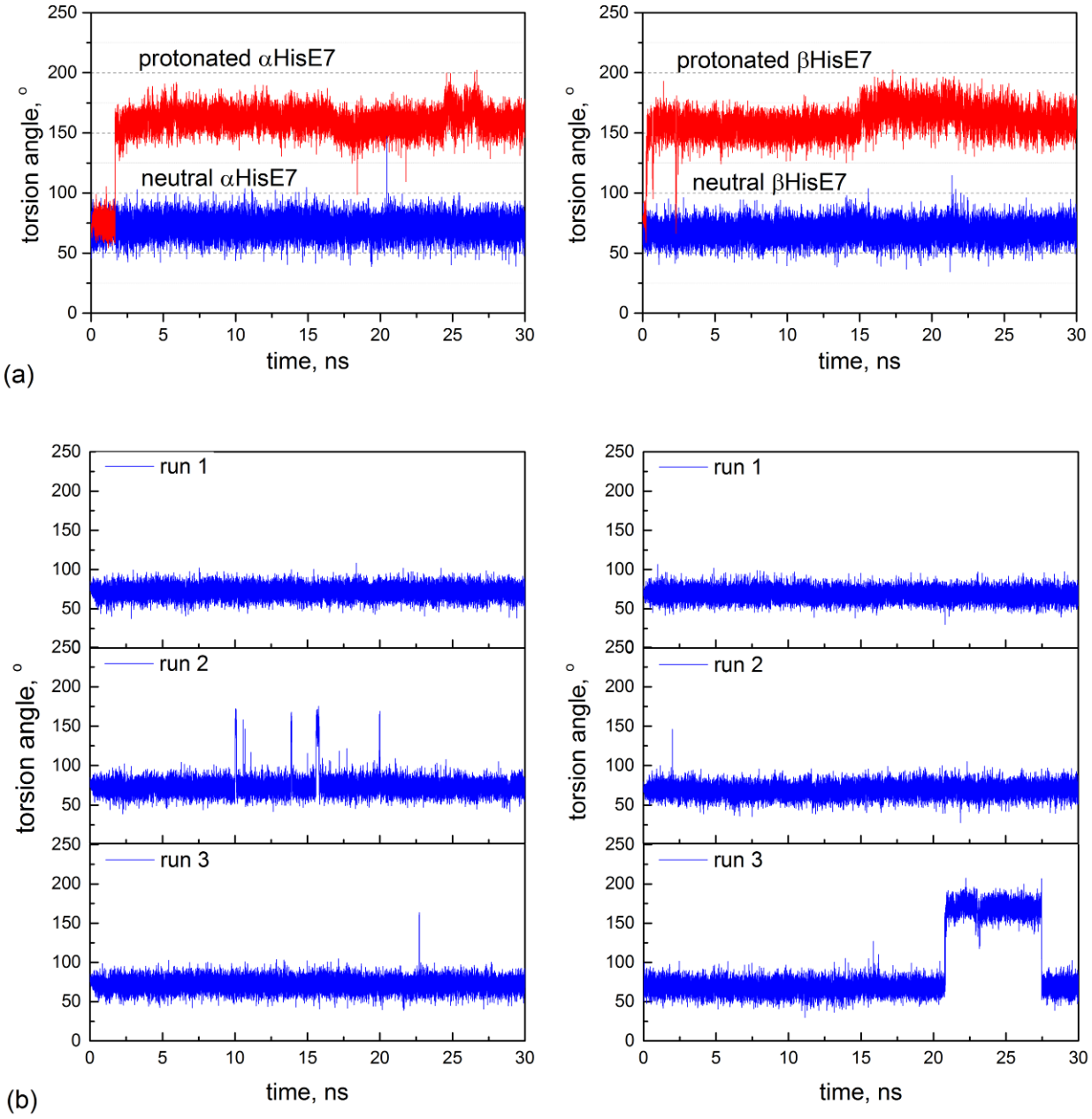

Figure S1. The HisE7 C-C_α-C_β-C_γ torsion angle vs simulation time for the R_c and R_o models. Torsion angles of ~70° and ~170° characterize the open and closed conformations of HisE7, respectively (see Figure 1 of the main text). Variation in the C-C_α-C_β-C_γ torsion angle during: (a) an arbitrary simulation of $\mathbf{R_c}$ (blue) and of $\mathbf{R_o}$ (red); and (b) three arbitrary simulations of the α-subunit (left panels) and β-subunit (right panels) of $\mathbf{R_c}$. Note that run 3 for the β-subunit exemplifies spontaneous opening of the neutral HisE7. The data shown are derived from ligand-free standard MD simulations (Table S1).

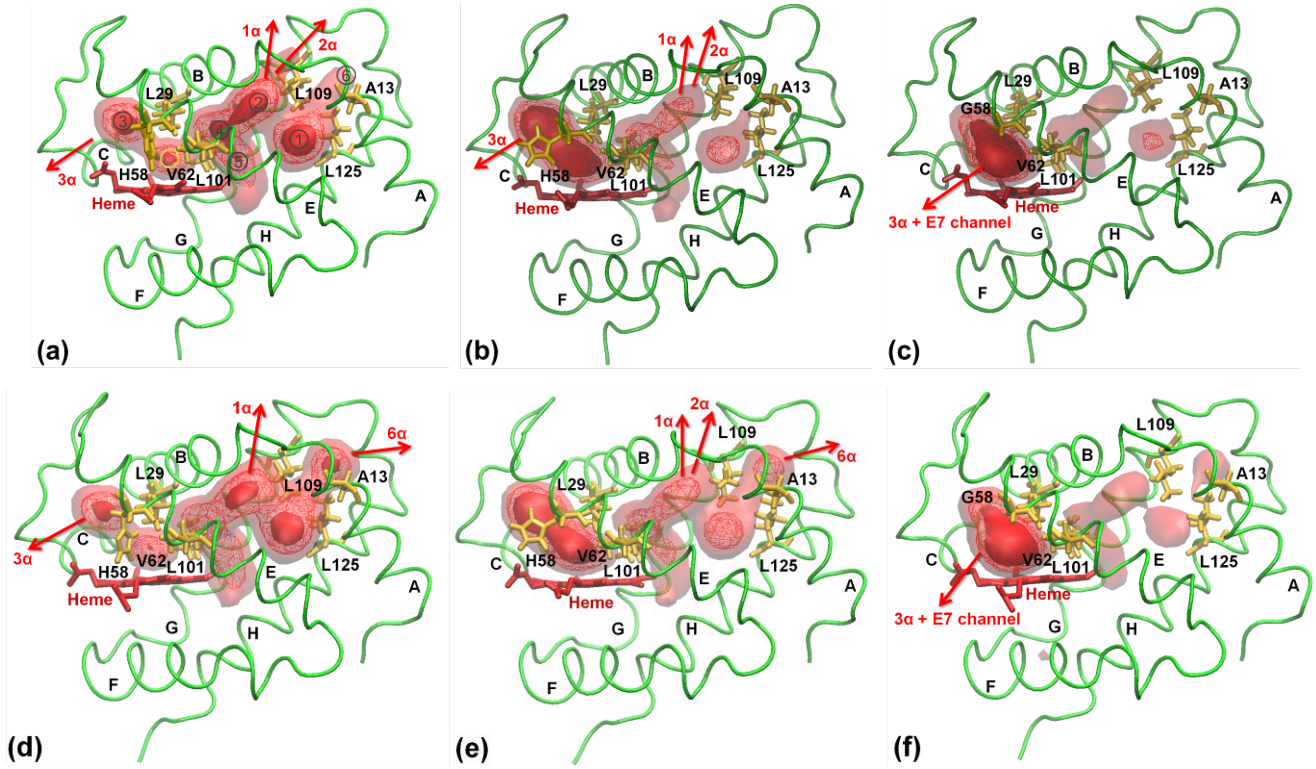

Figure S2. Maps of O_2 density within the kinetically accessible diffusion tunnels of the α-subunit of the six HbA models. Maps were plotted using 480 trajectories of TLES O_2 diffusion from the distal heme sites of the (a) $\mathbf{T_c}$, (b) $\mathbf{T_o}$, (c) **T**. (d) $\mathbf{R_c}$, (e) $\mathbf{R_o}$ and (f) **R**. models. Isosurfaces define regions with ≥0.5% (solid), ≥0.1% (wireframe), ≥0.025% (transparent) average occupancy during the simulations. Ribbons represent the backbone atoms of the α-subunit. The heme is shown as red stick, and the E7 residue (H58, αG58), the B10E11G8 barrier (residues αL29, αV62, αL101) and the α-barrier G16H8A11 (residues αL109, αL125, αA13) are shown as amber sticks. The yellow circle in (a) indicates the distal site, and the black circles locate the experimental Xe docking sites observed in the crystals of HbA and HbYQ.(*3*) The arrows locate the major O_2 exit portals from the α-subunit, including those from the interior tunnels (Table 1 of the main text).

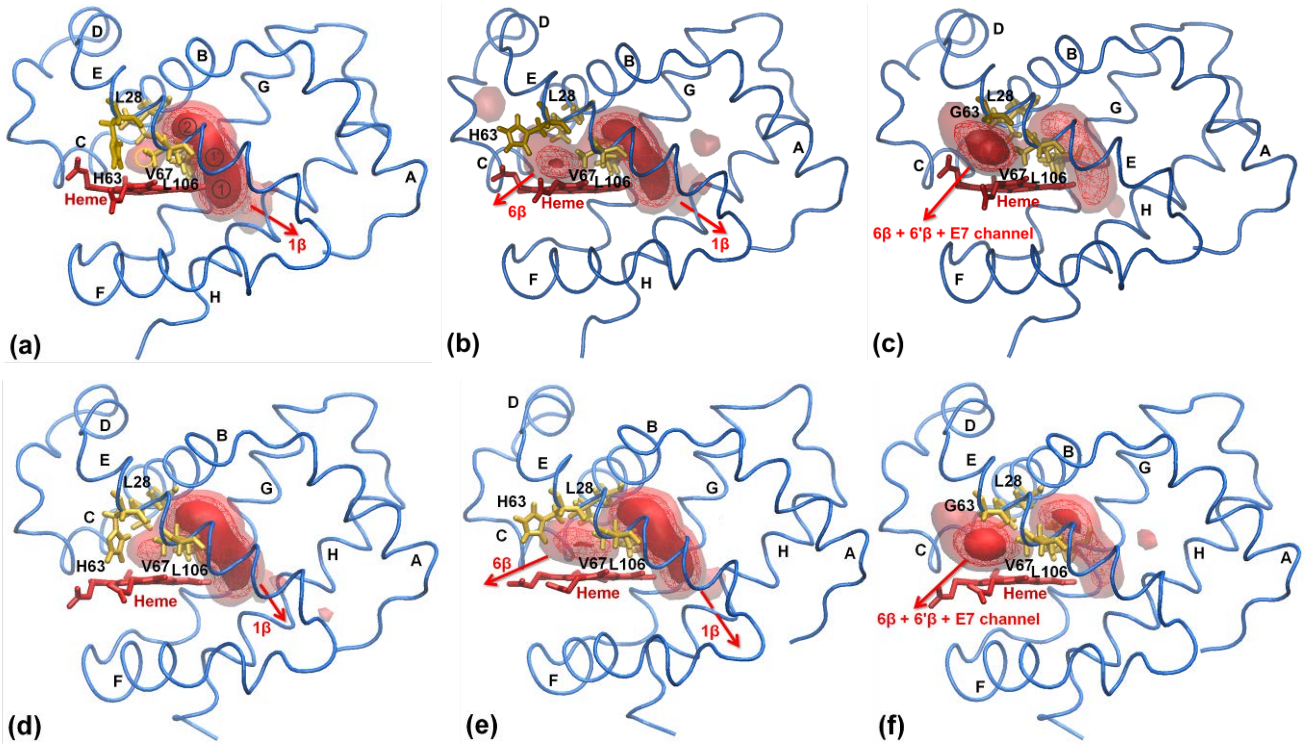

Figure S3. Maps of O_2 density within the kinetically accessible diffusion tunnels of the β-subunit of the six HbA models. Maps were plotted using 480 trajectories of TLES O_2 diffusion from the distal heme sites of the (a) $\mathbf{T_c}$, (b) $\mathbf{T_o}$, (c) **T**. (d) $\mathbf{R_c}$, (e) $\mathbf{R_o}$ and (f) **R**. models. Isosurfaces define regions with ≥0.5% (solid), ≥0.1% (wireframe), ≥0.025% (transparent) average occupancy during the simulations. Ribbons represent the backbone atoms of the β-subunit. The heme is shown as red sticks, and the E7 residue (H63, βG63) and the B10E11G8 barrier (residues βL28, βV67, βL106) are shown as amber sticks. The yellow circle in (a) indicates the distal site and the black circles locate the experimental Xe docking sites observed in the crystals of HbA and HbYQ.(*3*) The arrows locate the major O_2 exit portals (Table 2 of the main text).

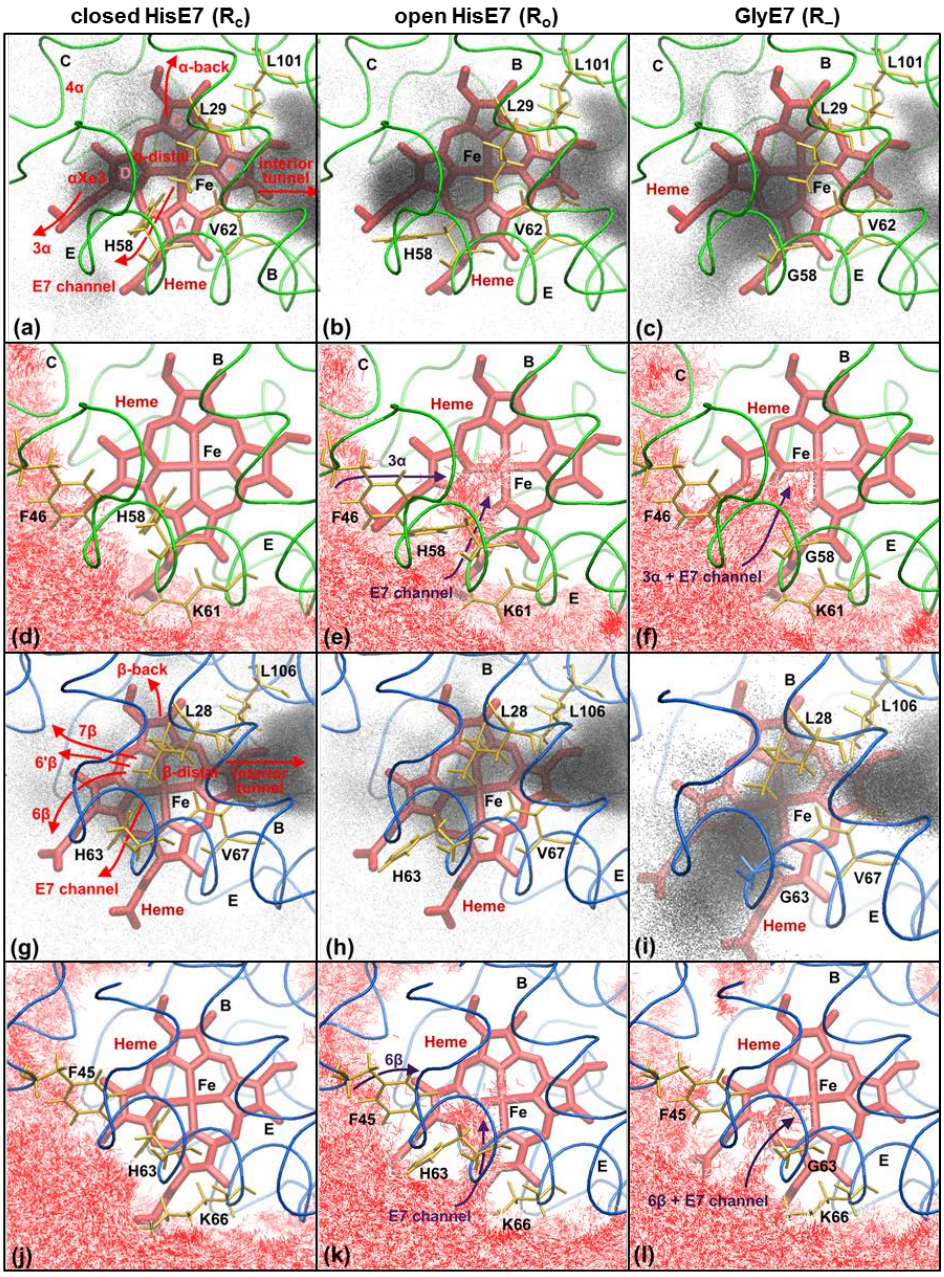

Figure S4. O_2 and water distribution around the heme of the α-subunit (green) and β-subunit (blue) of the R_c, R_o and R_- models viewed from the distal side. (a–c, g–i) Black dots represent O_2 positions derived from 480 trajectories of TLES O_2 diffusion from the α- and β-distal sites labeled in panels a and g. (d–f, j–l) represent the water positions observed during a 0.5-ns window of ligand-free standard MD simulations (Table S1). The key distal residues that control O_2 and water access to the heme, E7 (αH58, βH63, αG58 or βG63), PheCD4 (αF46, βF45) and LysE10 (αK61, βK66) as well as the B10E11G8 barrier between the heme and the interior tunnels (residues αL29, αV62, αL101 or βL28, βV67, βL106) are shown as amber sticks. Red arrows (panels a,g) indicate all observed O_2 escape routes from the heme distal pockets, and the frequency of portal use is summarized in Tables 1 and 2 of the main text. The rotation of HisE7 toward the solvent allows extensive water access via the E7 channel and minor paths, which are marked by purple arrows in panels e,k. Plots for the $\mathbf{T_c}$, $\mathbf{T_o}$ and $\mathbf{T_-}$ models are shown in Figure 2 of the main text.

References for Supporting Information

1. Chatake, T., Shibayama, N., Park, S. Y., Kurihara, K., Tamada, T., Tanaka, I., Niimura, N., Kuroki, R., and Morimoto, Y. (2007) Protonation states of buried histidine residues in human deoxyhemoglobin revealed by neutron crystallography, *J. Am. Chem. Soc. 129*, 14840-14841.
2. Park, S. Y., Yokoyama, T., Shibayama, N., Shiro, Y., and Tame, J. R. (2006) 1.25 A resolution crystal structures of human haemoglobin in the oxy, deoxy and carbonmonoxy forms, *J. Mol. Biol. 360*, 690-701.
3. Savino, C., Miele, A. E., Draghi, F., Johnson, K. A., Sciara, G., Brunori, M., and Vallone, B. (2009) Pattern of cavities in globins: the case of human hemoglobin, *Biopolymers 91*, 1097-1107.